2016-02-01

Structural Dependence of the In Vitro Cytotoxicity, Oxidative Stress and Uptake Mechanisms of Poly(propylene imine) Dendritic Nanoparticles

Humza Khalid
Technological University Dublin

Sourav Prasanna Mukherjee
Technological University Dublin

Luke O'Neill
Technological University Dublin, Luke.oneill@tudublin.ie

Hugh Byrne
Technological University Dublin, hugh.byrne@tudublin.ie

Recommended Citation

Byrne, H. et al. (2016) Structural dependence of the In vitro cytotoxicity, oxidative stress and uptake mechanisms of Poly(propylene imine) dendritic nanoparticles", *Journal of Applied Toxicology,* 36, 464-473 (2016). doi:10.1002/jat.3267

Structural dependence of the I*n vitro* cytotoxicity, oxidative stress and uptake mechanisms of Poly(propylene imine) dendritic nanoparticles.

Humza Khalid[*1,2], Sourav Prasanna Mukherjee[3], Luke O'Neill[1] and Hugh J. Byrne[1].

[1] FOCAS Research Institute, Dublin Institute of Technology, Kevin Street, Dublin 8, Ireland,
[2] School of Physics, Dublin Institute of Technology, Kevin Street, Dublin 8, Ireland,
[3] Institute of Environmental Medicine (IMM), Karolinska Institute, Stockholm, Sweden

*Corresponding Author: hugh.byrne@dit.ie

Abstract

The *in vitro* cytotoxic and intracellular oxidative stress responses to exposure to poly (propylene imine) (PPI) dendritic nanoparticles of increasing generation (number of repeated branching cycles) (G0-G4) were assessed in an immortal non-cancerous human keratinocyte cell-line (HaCaT). Confocal fluorescence microscopy with organelle staining was used to explore the uptake and intracellular trafficking mechanisms. A generation and dose dependent cytotoxic response was observed, increasing according to generation and therefore number of surface amino groups. A comparison of the cytotoxic response of G4 PPI and the related G4 Poly (amido amine) dendrimer indicates that the PPI with the same number of surface amino groups elicits a significantly higher cytotoxic response. The trend of cytotoxicity versus dendrimer generation and therefore size is discontinuous in the region of G2, however, indicating a difference in uptake mechanism for higher compared to lower generations. Whereas the higher generations elicit an oxidative stress response at short exposure times, the lower generations indicate and antioxidant response. Confocal microscopy indicates that, whereas they are prominent at early exposure times for the larger PPI dendrimers, no evidence of early stage endosomes was observed for lower generations of PPI. The results are consistent with an alternative uptake mechanism of physical diffusion across the semi-permeable cell membrane for the lower generation dendrimers and are discussed in terms of their implications for predictive models for nanotoxicology and design strategies for nanomedical applications.

Keywords: Poly(propylene imine) dendrimers, Poly(amido amine) dendrimers, cytotoxicity, oxidative stress, *in vitro* uptake mechanisms, structure property relationships

1. Introduction

The production of engineered nanoparticles has significantly increased over the last decade, in line with the prediction of a shift from basic nanoparticle research and development to mass production by 2015 (Project on Emerging Nanotechnologies, 2015). Today, nanoparticle applications encompass every aspect of our lives, from fertilizers (Liu and Lal, 2015) and fuel (Dahle and Arai, 2015) to medicine (Parat et al., 2015). Concomitant with the increase in nanoparticle applications is the continuing study of their potential impacts on the environment and human health and the recognition of the need for systematic testing strategies and a greater understanding of the relationship between nanoparticle physico-chemical structures and biological activity (Lynch et al., 2013, Oomen et al., 2014). Understanding the mechanisms of cellular interactions will aid the

development of nanoparticles with properties that will maximise efficacy and minimise non-specific toxicological responses. Furthering our knowledge of intracellular mechanisms will assist the betterment of nanomedicine and more specifically drug delivery.

The last decade of research has identified the beneficial application of polymers on the nanoscale of 5-100 nm and, in this context, dendritic nanostructures feature highly (Duncan and Izzo, 2005). The ability to control the size, shape and surface functionality has attracted many to exploit these characteristics and potential usage in nanomedical applications (Dear et al, 2006, Guillot-Nieckowski et al., 2007, Swanson et al., 2008, Na et al., 2008, Sha et al., 2011). Dendrimers are 3-D branched polymeric particles of nanometer scale. With increasing generation (number of repeated branching cycles), both the size and surface structure is systematically varied. The dendrimer poly (propylene imine) (PPI) is a well-defined, highly branched molecule (Tomalia, 2005). It possesses a diaminobutane core and successive generations have increasing number of surface functional groups. In the case of poly (propylene imine) (PPI) and the related family poly (amido amine) (PAMAM) dendrimers (Tomalia, 2005), the surface functional groups are polarised primary amino groups, resulting in an effective cationic surface charge The surface groups provide excellent solubility that ensures their stability and dispersion in aqueous solutions (Tomalia, 2005). Notably, increasing dendrimer generation provides a route towards systematic variation of nanoparticle physico-chemical properties.

Polymeric dendrimer systems have been proposed for a range of biomedical applications, from magnetic resonance imaging contrast agents (Bourne et al., 1996), to targeted-delivery of drugs (Ywyman et al., 1999), DNA (Guillot-Nieckowski et al., 2007) and small interfering RNA (siRNA) (Zhou et al., 2006). In the field of therapeutics, dendrimers constitute an important class of drug delivery vehicles (Kannan et al., 2006, Pignatello et al., 2009, Kesharwani et al., 2014, Kesharwani and Iyer 2015). They may potentially be used to covalently bind and physically entrap drug molecules to improve their water solubility, decrease their toxicity, increase their permeability and the affinity for their target (Najlah et al. 2006).

Notably, in terms of understanding nanoparticle cell interactions which can govern cytotoxic responses and intercellular trafficking mechanisms, important for optimised drug delivery, such homologous series of structurally well-defined nanoparticles can also play a critical role (Mukherjee and Byrne, 2010, Mukherjee et al., 2010, Naha et al, 2010, Mukherjee and Byrne, 2013). Although it has been demonstrated that dendrimer toxicity can be minimised by appropriate surface modification (Cheng et al., 2011, Wang et al., 2012), study of the precise and systematically variable basis structures can add much to the understanding of the dependence of the cellular interactions and responses on the physico-chemical properties of nanoparticles, which in turn may lay the foundation for quantitative structure property relationships and predictive models.

In this context, PAMAM dendrimers have been extensively studied to understand the mechanisms of cellular interaction *in vitro* (Kitchens et al., 2008, Lee et al. 2009, Mukherjee and Byrne, 2010, Mukherjee et al., 2010, Naha et al, 2010, Mukherjee and Byrne, 2013). Mukherjee et al. identified that the toxic response is dependent on generation and dose, the nanoparticles becoming more toxic with increasing generation (size) (Mukherjee and Byrne, 2010). A strong correlation has been identified between toxicity and intracellular reactive oxygen species (ROS) production (Naha et al, 2010,

Mukherjee and Byrne, 2013). A biphasic increase in ROS was observed, the initial increase of ROS being attributed to the active uptake of the dendrimer by the process of clatherin mediated endocytosis (Kitchens et al., 2008, Mukherjee et al., 2013). The second increase of ROS is due to localization of the PAMAM at the mitochondria via the mitochondrial injury pathway (Xia et al, 2006). The early stage responses to PAMAM exposure have been modelled using a rate equation response, demonstrating that the time, dose and generation dependent cytotoxic responses could be predicted using the single parameter of number of surface amino groups, while the dependence on cytotoxic assay and cell type was faithfully reproduced by considering the different timescales of the endpoints, and the protective effect of intracellular antioxidants, respectively (Mukherjee et al., 2013, Maher et val., 2014).

While it has been identified that polymeric dendrimer nanoparticles elicit a significant cytotoxic response (Nel et al. 2006, Naha et al, 2010, Mukherjee and Byrne, 2010, Mukherjee et al., 2010, Mukherjee and Byrne, 2013), precise structure activity relationships are still to be elucidated. PPI and PAMAM dendrimers have similar outer structures of surface amino groups but different cores, and therefore different overall dimensions. Comparison of the chemically analogous but physically distinct nanoparticles can add to the understanding of the dependence of the uptake on the particle size. Furthermore, extension of the study from the higher and intermediate dendrimer generations to lower generations addresses the fundamental questions of the difference between large molecules and nanoparticles in terms of cellular uptake mechanisms.

In this study, the toxic response to and interaction mechanisms of PPI dendrimers G0 – G4 (using the nomenclature of Tomalia and Rookmaker, 2009, and Kesharwani et al., 2015) were examined in HaCaT, human keratinocyte cells, as a model for dermal interactions as well as for intercomparison with previous studies. Cellular toxicity was determined by the MTT (3-[4,5-Dimethylthiazol-2-yl]-2,5-diphenyl tetrazolium bromide) assay, which determines the mitochondrial activity of viable cells, and which has previously been demonstrated to be the most sensitive amongst tested cytotoxicity assays (Neutral Red, Alamar Blue, MTT) (Mukherjee and Byrne, 2010, Naha et al, 2010, Maher et al., 2014). To further understand the mechanism of toxicity of PPI dendrimers, ROS production was assessed on a subcellular level, as previous mechanistic studies which monitored oxidative stress, mitochondrial membrane potential and inflammatory markers (caspase 3, 8, TNF-α), have indicated that ROS generation is an early quantitative indicator of toxic response (Naha et al., 2010, Mukherjee and Byrne 2013, Naha and Byrne 2013, Maher et al., 2014). The results are qualitatively and quantitatively compared to previous observations of HaCaT cells exposed to PAMAM dendrimers (Mukherjee et al., 2010, Mukherjee and Byrne 2013), in order to evaluate the importance of the structural variations between the two dendrimer series. The results indicate a similarity of uptake mechanism and cytotoxic response, via a biphasic oxidative stress profile, for the larger generations of PPI and PAMAM. However, a transition from a regime of active uptake of the larger dendrimers by endocytosis, to one of passive uptake of the smaller ones, by physical diffusion across the semi-permeable membrane, is indicated. It is shown that the passive uptake of the smaller dendrimers results in significantly lower oxidative stress and cytotoxicity, suggesting that understanding how

nanoparticles cross cell barriers e.g. cell membrane, can greatly benefit the targeting of nanoparticles as drug delivery vehicles.

2. Methods and Materials

2.1 Test Materials

PPI dendrimers were obtained from Symo-Chem BV (Eindhoven, Netherlands). PPI dendrimers generation 0 (G0), 1 (G1), 2 (G2), 3 (G3), 4 (G4) have 4, 8, 16, 32 and 64 primary surface amine group, respectively. The molecular weights of PPI G0, G1, G2, G3 and G4 are 316.5 Da, 773.3 Da, 1686.8 Da, 3513.9 Da and 7168.1 Da, respectively. The dendrimers are readily soluble in water and G0, G1, G2, G3 and G4 stock solutions of respective concentrations 6000µM, 500µM, 30mM, 9mM and 3.5mM were prepared in Milli Q deionised water and cell culture medium. These stock solutions were then serially diluted to generate the concentration ranges for the dose dependent measurements of cell viability and oxidative stress. PPI nanoparticles were tested for interferences with the respective assays, by acellular tests of the assays in the presence of nanoparticles at their highest concentrations and none were found. Fluorescently labelled 40nm polystyrene nanoparticles (PSNPs) were purchased from BioSciences (Dun Laoghaire, Ireland) and made up to 1 x 10^{12} particles/ml in cell culture medium as a control for endosomal detection.

Both the PPI and PAMAM dendrimers used are commercially available, and their synthesis is well established. Size analysis was conducted using dynamic light scattering and atomic force microscopy as a confirmation of particle dispersion and aggregation state. The details of the methods are described in detail in the Supplemental Information.

2.2 Cell culture

The HaCaT cell line, an immortal non-cancerous human keratinocyte cell line, was used to evaluate the cytotoxicity of the PPI dendrimers. HaCaT cells were obtained from Cell Line Services (Eppelheim, Germany). They were passaged at 70-80% confluence and cells did not exceed 15 passages. HaCaT cells were cultured in Dulbecco's modified eagle medium (DMEM, Sigma Aldrich, Arklow, Ireland), Nutrient Mixture F-12, with 2 mM L-glutamine supplemented with 5% Foetal Bovine Serum (FBS), 45 IU ml^{-1} penicillin, 45 IU ml^{-1} streptomycin (all from BioSciences, Dun Laoghaire, Ireland) and 1µg/ml hydrocortisone (Sigma Aldrich, Arklow, Ireland) at 37 °C in 5% CO_2.

2.3 Cytotoxicity

The MTT (Sigma Aldrich, Arklow, Ireland) assay was used to measure cell viability. The assay is based on measurement of the activity of the mitochondria, which is constant in viable cells and therefore an increase or decrease in viability as a result of nanoparticle exposure correlates to a change in the mitochondrial activity (van Meerloo et al., 2011). Cells were seeded at a density of 1 x 10^5 cells/ml in a 96 well plate in 100µl 5% FBS medium/well. After 24hr incubation at 37 °C in a 5% CO_2 incubator, the medium was removed and the cells were washed with 100µl phosphate buffered saline (PBS) and treated with dendrimer solutions of varying concentrations. Negative (medium without PPI) and positive controls (exposed to H_2O_2, an oxidizing agent used to cause oxidative damage within the cell) were also prepared. Three individual experiments were performed, each including six replicates for both controls and treatments. After 24hr of dendrimer exposure, the medium was removed from all wells and the cells were washed

with 100µl PBS. 100µl of 5mg/ml MTT dye in medium (without FBS or supplements) were added to each well. After 3hr incubation at 37 °C in an atmosphere of 5% CO_2, the dye was removed and the cells were washed with 100µl PBS and 100µl dimethyl sulphoxide (Sigma Aldrich, Dublin, Ireland) were added and the samples were shaken at 240 rpm for 10mins. The MTT absorbance was measured at 595nm using a TECAN GENios (Grodig, Austria) plate reader to determine the cell viability compared to the control.

2.4 Oxidative Stress

As a measure of oxidative stress, changes in ROS production upon exposure to PPI dendrimer nanoparticles were monitored using the Carboxy-H2DCFDA dye assay (BioSciences, Dun Laoghaire, Ireland) (Kehrer and Paraidathathu, 1992). The study was performed in black 96 well plates, and cells were seeded at 1 x 10^5 cells/well. The plates were incubated at 37 °C in a 5% CO_2 atmosphere. After 24hrs, each well was washed with 100µl PBS. Carboxy-H2DCFDA dye was added at a concentration of 10µM and plates were incubated at 37 °C in a 5% CO_2 for 1hr. Plates were then removed and washed 3 times with PBS at 100µl/well. Wells were treated with controls, positive (medium without PPI) and negative (H_2O_2), and treatments of G0- G4 PPI dendrimers prepared in 5% FBS containing media at varying concentrations. Experiments were performed in three independent experiments and each included six replicates of each treatment concentration. The fluorescence of the Carboxy-H2DCFDA dye was measured at time intervals 1-4, 6, 12 and 24hrs, at an excitation wavelength of 488nm and emission wavelength of 535nm using a TECAN GENios (Grodig, Austria) plate reader.

2.5 Confocal Microscopy

Commercially available PPI dendrimers are not fluorescent, and although several studies using fluorescently labelled dendrimer nanoparticles as intracellular probes have been reported, it is not clear that the transport mechanisms of (cationic) dendrimers fluorescently labelled with anionic moieties (FITC in the case of Kitchens et al., 2007 or Alexafluor in the case of Thomas et al., 2009) are the same as their unlabelled counterparts. For example, Gajraj and Ofoli (2000) have reported that extrinsic labelling of fluorescein-5-isothiocyanate (FITC) to bovine serum albumin (BSA) in a ratio of 2:1 changes its adsorption and diffusion properties. Confocal fluorescence microscopy was therefore employed to visualize and locate the increased ROS production, as well as the presence of early endosomes in HaCaT cells as a result of exposure to PPI dendrimers. To monitor ROS production, cells were seeded by adding 100µl of 1 x 10^5 cell suspension to the centre of a glass bottom Petri-dish. After 2hrs incubation at 37 °C in an atmosphere of 5% CO_2, 3mls of 10% FBS supplemented medium were added. Cells were incubated for 24hrs at 37 °C in 5% CO_2, where after they were treated with 2mls of 10µM Carboxy-H2DCFDA dye. The Petri-dishes were incubated for a further 45mins, and then the cells were treated with the appropriate concentration of PPI dendrimer (chosen to be close to the respective EC_{50} value) and incubated for a duration of 5hr or 24hr. At each time point, the Petri-dish was removed and the cells were washed twice with PBS. Mitotracker dye solution (BioSciences, Dun Laoghaire, Ireland) (Bhattacharyya et al., 1995) was prepared at 2µM in pre-warmed PBS and added to the cells for 30mins incubation at 37 °C in a 5% CO_2. After the staining, the cells were washed with PBS three times and 3mls of warm PBS was added. Experiments were

performed in three independent experiments and each included six replicates of each treatment concentration.

To examine the uptake mechanisms, fluorescently labelled PSNPs were used as a control, as they have previously been demonstrated to be taken up in cells by endocytosis and subsequently trafficked through endosomes and lysosomes (Ekkapongpisit et al. 2012, Sandin et al., 2012, Monti et al., 2015). The CellLight reagent (BioSciences, Dun Laoghaire, Ireland), a fluorescent protein-signal peptide fusion, was used to visualize the early endosomes. It uses BacMan technology, which uses an insect cell virus (baculovirus) coupled with a mammalian promoter (Kost and Patrick, 1999). Cells were seeded by adding 100µl of 1 x 10^5 cell suspension at the centre of a glass bottom Petri-dish. After 2hrs incubation at 37 °C in 5% CO_2, 3mls of 10% FBS supplemented medium were added. Cells were incubated for 24hrs at 37 °C in a 5% CO_2, after which they were treated with a solution containing 30 CellLight particles per cell (PPC). The Petri-dishes were incubated for a further 24hrs. The following day, the cells were washed with PBS and treated with the required concentration of PPI dendrimer, or PSNPs for control, and incubated for a duration of 5hrs. After 5hrs, cells were removed, washed twice with PBS and 3mls of warm PBS were added. Confocal images were taken using a Zeiss Confocal Fluorescence Microscope (LSM 510 META, Carl Zeiss, Jena, Germany).

2.6 Statistics

All experiments were conducted in triplicate (three independent experiments), each containing 6 replicates. Fluorescence as fluorescent units (FUs) of all of the assays was quantified using a TECAN microplate reader (TECAN GENios, Grödig, Austria). Control values were set at 100%.

Toxicity data was fitted by a sigmoid curve and a four parameter logistic model was used to calculate EC_{50} values. This analysis was performed using Xlfit3™, a curve fitting add-in for Microsoft® Excel (ID Business Solutions, Guildford, UK). ROS data was analysed using Microsoft Excel® (Microsoft Corporation, Redmond, USA). ROS data was expressed as mean percentage viability in comparison to the unexposed control (100%) ± standard deviation (SD).

3. Results

3.1 Physico chemical properties

As recommended, the physico-chemical properties of the test species were characterised (Bouwmeester et al., 2011). Full details of the characterisation of PPI G0 – G4 determined by Atomic Force Microscopy are presented in the supplementary information. The particle size measurements for the PPI dendrimer series are tabulated in Table 1. The measured particle sizes are consistent with manufacturer's specifications. However, PPI dendrimers G0 and G1 are clearly present as aggregates in aqueous suspension at concentrations above of >1000µM for G0 and >500µM for G1.

3.2 Cytotoxicity

As shown in figure 1, a dose and generation dependant cytotoxic response in HaCaT cells, as determined using the MTT assay after 24 hr exposure was observed, G4 producing the highest toxic response and G0 the lowest response. This correlates well with the variation in the number of surface amino groups present on the surface of the

dendrimer and strongly suggests a systematic structure activity relationship governing the toxic response of PPI dendrimers. For all generations, a dose dependent response is apparent, and the degree of toxicity increases systematically with generation, consistent with a mechanism which is dependent on the number of surface amino groups, as indicated for the related PAMAM dendrimer series (Mukherjee and Byrne, 2010, Mukherjee et al., 2010, Naha et al, 2010, Mukherjee and Byrne, 2013, Maher et al., 2014). For PPI G1, negligible cytotoxic response is observed at doses <100μM, above which dose, the toxic response is seen to increase rapidly. A similar behaviour is observed for PPI G0, above 1000μM. In comparison with the dose dependent cytotoxic response of the higher dendrimer generations, G2-G4, the dose dependence of the response is very steep. It should be noted that aggregation of particles, itself a dose dependent phenomenon, was observed at concentrations of >1000μM for G0 and >500μM for G1, indicating that the rapid decrease in cell viability is due to exposure to aggregates of PPI G0 and G1 (supplemental material, Figure S7, S8).

3.3 Oxidative Stress

In the case of the PAMAM dendrimer series, the generation dependent toxic response has origin in a similarly generation dependent oxidative stress response and this response has a complex dependence on the dose and time (Mukherjee and Byrne, 2010). Studies of PAMAM G4-G6, revealed a dose and time dependent biphasic ROS generation process (Mukherjee and Byrne, 2010, Mukherjee et al., 2010, Naha et al, 2010, Mukherjee and Byrne, 2013, Maher et al., 2014). The early phase (2-6hr) increase in ROS levels compared to control was associated with early stage intracellular trafficking in endosomes, whereas the later stage has been associated with localisation of the dendrimers in mitochondria (Xia et al., 2006, Lee et al., 2009, Mukherjee et al., 2010). To better understand the structural dependence of the PPI toxic responses, it is thus important to consider the time and dose dependence of the ROS generation in the HaCaT cell line.

The ROS study is consistent with a similar, although less pronounced, biphasic increase of ROS in HaCaT cells for the higher generations, as exemplified for the case of G4 in figure 2. For the case of 1.5μM exposure, an initial increase was observed after approximately 5hrs of exposure. This initial increase was seen to subside within approximately 6hrs exposure, after which a further continuous increase was observed, up to the maximum exposure time of 24hrs. Generations G3 and G2 exhibit similar behaviour to G4 (not shown). In contrast, PPI generations G0 and G1 are seen to induce a strongly antioxidant response, reducing the intrinsic ROS levels to as low as <60% of the control values in the case of PPI G0. The level of quenching of the intrinsic ROS reduces with increasing time, however. The response to G2 and G3 exposure appears to be intermediate between the extremes of oxidative stress for G4 and antioxidant behaviour for G0 (data not shown).

In the case of PPI G0 and G1, the longer time increase in ROS levels may be similarly associated with localisation of the dendrimers in the mitochondria, but the absence of the early stage endosomal ROS suggests an alternative uptake mechanism to endocytosis, by which the internalised G0 and G1 dendrimers act as antioxidants.

3.4 Confocal Microscopy

The study of the cytotoxic and oxidative stress responses of HaCaT cells to exposure to PPI dendritic nanoparticles indicated a clear similarity to those previously documented for PAMAM dendrimers (Mukherjee et al., 2010, Mukherjee and Byrne 2013). Notably, the biphasic response of the ROS for the higher generations is similar to that observed for PAMAM dendrimer exposure, attributed to a process of endocytosis and early stage ROS production due to the endosomal proton pump mechanism, followed by endosomolysis and subsequent localisation of the dendrimers and ROS production in the mitochondria (Nel et al., 2009, Mukherjee et al., 2010). In order to confirm a similar mechanism as origin for the biphasic ROS response to PPI exposure, an investigation of colocalisation of the early and late stage ROS with the mitochondria was performed. An overlap of Carboxy H_2DCFDA (yellow) and the mitotracker dye (red) producing an orange shade indicates the presence of ROS in the mitochondria.

Figure 3 depicts exposure of 20µM PPI G2 at the early maximum ROS of approximately 5hrs and late stage of ROS at 24hrs. The dominance of the red fluorescence of the mitotracker dye in (Figure 3a) indicates that no ROS was present in the mitochondria at 5hr exposure, whereas a significant ROS production was seen to be located in the mitochondria at 24hrs (Figure 3b). In general, after 24hrs exposure of HaCaT cells, a significant production of ROS was observed in the mitochondria for the case of each PPI dendrimer generation. Figure S10 shows a similar image for 24hr exposure for the example of 2µM of PPI G4.

The presence of early endosomes after the treatment of HaCaT cells with PPI dendrimers was examined using the CellLight reagent. Fluorescently labelled 40nm PSNPs were used as a positive control, as previous literature has shown that they are taken into cells by the active uptake of endocytosis (Nel et al., 2009, Sandin et al., 2012, Ekkapongpisit et al. 2012, Monti et al., 2015). Figure S11 confirms the endocytosis of polystyrene nanoparticles after 5hr exposure; the fluorescently labelled nanoparticles are shown in green and the red dye shows the presence of early endosomes. The significant overlap of the two indicated by the orange colour in Figure S11 (d), confirms that the polystyrene nanoparticles are localised in early endosomes.

In a similar way, early endosomes are clearly detectable by the red fluorescence of the CellLight dye after 5hr exposure of HaCaT cells to PPI dendrimers, as shown in Figure 4, for the example of 0.3µM PPI G4 dendrimer solution. Exposure of HaCaT cells after 5hrs to PPI G0 and G1 showed no sign of early endosomes, however, as shown in Figure 5 for the example of 1000µM PPI G0, in which no red fluorescent CellLight dye is detectable. A similar examination of early stage exposure of HaCaT cells to PPI G1 dendrimer solutions failed to detect any early stage endosomal activity (not shown), indicating the absence of an active uptake of the smaller PPI dendrimers.

4. Discussion

The cytotoxicty of PPI dendrimers was determined by the MTT assay. A generation and dose dependent toxic response was observed, in the order of G0<G1<G2<G3<G4. The cytotoxicity of the related family of PAMAM dendrimers has been extensively studied (Heiden et al., 2007, Lee et al., 2009, Mukherjee and Byrne, 2010, Mukherjee et al., 2010, Naha et al., 2010, Mukherjee and Byrne, 2013, Naha and Byrne, 2013). The responses have been similarly seen to increase with increasing generation and to be correlated with the number of surface amino groups. Figure 6 compares the variation of

EC_{50} of PAMAM G4 to G6 (values reproduced from Mukherjee et al., 2010) and PPI G0 to G4, in both cases measured by the MTT assay in the HaCaT cell line after 24hrs exposure. As the degree of toxicity is inversely related to the magnitude of the EC_{50} measured, the results are plotted as inverse (Ragnvaldsson et al. 2007). The EC_{50} values are listed along with physico-chemical parameters in Table 1.

In the case of each dendrimer series, a dependence of the toxic response, as represented by the inverse EC_{50} measured using the MTT assay at 24hrs, on the number of surface amino groups is clearly seen. It has previously been proposed that the toxic response of dendritic nanoparticles is governed primarily by the number of surface amino groups (Mukherjee et al., 2010, Maher et al. 2014). A clear correlation between the toxic response and the number of surface amino groups is evident for both the PAMAM and PPI series, although the trend for the latter deviates sharply from linearity at the lower generation, G2. The inverse EC_{50} values of PPI show them to be relatively more toxic than PAMAM. For example, PPI G4, with the same number of surface amino groups as G4 PAMAM, is two to three fold more toxic.

Comparative studies between PPI and PAMAM have previously been presented. Janaszewska et al. compared PPI G4 and PAMAM G4 and identified a rapid linear decrease in cell viability in Chinese hamster ovary (CHO) and human ovarian carcinoma cells lines over the concentration range of 0.1-10μM for both dendrimers (Janaszewska et al., 2012). The dendrimers displayed an insignificant difference in reduction of cell viability, although PPI G3 has half as many (32) surface amino groups as its PAMAM G4 counterpart (64). However, a previous cytotoxicity study by Shao et al. (2011), showed PPI G2 with 16 surface amino groups to be more toxic than PAMAM G4 with 64 surface amino groups, even though PAMAM G4 has 3 times more surface amino groups.

In considering differences in cytotoxicity endpoints, however, it is important to consider the mechanisms of response, which in the case of PAMAM dendrimers is reported to be due to oxidative stress after clathrin mediated endocytosis (Kitchens et al. 2008). A biphasic increase in ROS has been observed, the first phase (1-6hrs) associated with the endosomal proton pump mechanism and endosomolysis (Nel et al., 2006, Varkouhi et al., 2011), the second (~16-24hrs) associated with dendrimer localization and ROS production in the mitochondria (Lee et al., 2009, Mukherjee et al. 2010, Naha et al., 2010). A similar biphasic ROS response is observed for exposure to the higher PPI generations, G3 and G4, and the co-localisation of ROS in the mitochondria after 24hours is a strong indication that a similar mechanism governs the oxidative stress and cytotoxic response to PPI dendrimers. However, there is a significant disconnect between the trend shown by the higher PPI generations, G3-G4, and the lower generations (G0-G2), the latter group eliciting substantially lower responses. Notably, up to concentrations of ~100μM, cells treated with PPI G1 showed little toxicity and only above ~100μM did the viability decrease rapidly. Similarly, PPI G0 elicited little or no toxic response in cells until concentrations above ~1000μM.

Figure 7 shows the %ROS compared to control measured using the Carboxy-H2DCFDA dye assay at the time point of the early ROS maximum and a dose of 1.0μM, for both the PPI and PAMAM dendrimer series (Mukherjee and Byrne 2010, Mukherjee et al., 2010). The trend of ROS matches well that of the toxicity as a function of number of surface amino groups, illustrated in figure 7, except for the lower generations of PPI, G0- G2. In contrast, the trends of the late stage ROS versus number of surface amino groups show

little correlation to the toxicity, as shown in Figure S9. The correlation of Figure 8 for the larger generations of PPI and PAMAM dendrimers indicates that, once internalised in the cells, the early stage ROS is the primary source of the cytotoxic response after 24hrs, and that for each dendrimer series, a similar degree of early stage oxidative stress results in similar toxicity.

Nevertheless, figure 6 indicates a difference between the two series, the higher generation PPI dendrimers eliciting a higher toxic response than the PAMAM series, and for the PPI dendrimers, the lower generations elicit a lower toxic response. Recent studies have explored the mechanism of PAMAM toxicity to the human keratinocyte, HaCaT, cell line and modelled the observed responses according to a phenomenological rate equation model (Mukherjee and Byrne 2013, Maher et al., 2014). The model was successful in simulating the observed temporal and generation dependent responses, and was seen to be extendable to murine macrophages (J774A.1) and human colon cells (SW480). The simulated uptake of PAMAM dendrimers was seen to be generation (or size) dependent, and translating the model to the PPI series, the observed higher levels of ROS generation and toxic response are consistent with a higher rate of internalisation of the PPI G3 and G4 dendrimers, which are substantially smaller in diameter than their PAMAM counterparts, according to literature values (Crooks et al., 2001). However, within a series, the diameter is only slowly varying as a function of generation. Once internalised, the reactivity resulting in increased levels of ROS, is dependent on the number of surface amino groups per dendrimer.

The lower PPI generations appear to show distinctively different response, both in terms of toxicity and oxidative stress. Notably, ROS production by PPI G0-G2 was below that of the control at 4hr exposure. Salvati et al. demonstrated that the uptake of smaller molecules in a passive process, and occurs at rates significantly lower than that of nanoparticles (Salvati et al., 2011). This may indicate that PPI G0-G2, due to their small size, are taken up by an alternative internalization mechanism and avoid encapsulation in endosomes in which early ROS is produced. The clathrin mediated endocytosis pathway is generally accepted as the uptake mechanism for dendrimers (Kitchens et al., 2008). However, it should be noted that in the study of Kitchens et al, for PAMAM G2 dendrimers, localisation correlations of only ~50% were observed with clathrin markers after 0-1hr, indicating the co-existence of alternative uptake mechanisms. For example, in their study, Saovapakhiran et al. (2009) concluded that that internalization of PAMAM G3 dendrimers involved both caveolae-dependent endocytosis and macropinocytosis pathways. Furthermore, chlorpromazine, an inhibitor of clathrin assembly-disassembly (Wang et al., 1993) had no effect on the internalization of PAMAM dendrimers in A549 cells (Perumal et al., 2008).

Confocal microscopy of HaCaT cells exposed to PPI G0 and G4 for 5hrs provides strong evidence that the smaller PPI dendrimers are not taken up by an active endocytotic mechanism, as is the case for the larger PPI and PAMAM counterparts. Similar studies have clearly demonstrated that such an endocytotic pathway is active of the uptake of PPI and PAMAM dendrimers (Kitchens et al. 2008, Perumal et al., 2008), as well as a range of nanoparticles, including PS NPs (Ekkapongpisit et al. 2012, Sandin et al., 2012, Monit et al., 2015), used in this study as a control. In the case of cationic nanoparticles such as PPI and PAMAM dendrimers within the acidifying environment of endosomes, it is reported that the unsaturated surface amino groups sequester protons via the proton pump

mechanism, leading to early stage oxidative stress as a primary cause of cytotoxicity (Nel et al., 2009).

However, in the absence of endocytotic uptake, molecules that possess positive amino groups are generally regarded as scavengers of ROS. As examples, in a study conducted by Mozdzan et al. (2006), spermine and spermidine both demonstrated the ability to reduce Fe^{3+} to Fe^{2+}, and the ferric reducing activity of these molecules has been identified as a measure of anti-oxidant potential (Lotito and Frei, 2004). Carnosine, an endogenous dipeptide, has been shown to scavenge both reactive oxygen and nitrogen species (Hipkiss, 2009).

The transport of molecules and particles into the cell can happen in many ways. Generally it is considered that particles and nanoparticles are taken up by an active endocytoytic process which requires energy to be moved across the cell membrane. Salvati et al. (2011) demonstrated, however, that the uptake rate and therefore mechanism of dye molecules by cell is very different than that of nanoparticles, and notably does not require energy activation. Passive uptake by physical diffusion across the semi-permeable cell membrane is considered the mode of transport of molecules which can diffuse past the cellular membrane due to their small size, without the need for an internal energy source.

The study of the generation dependent response of the cytological responses to exposure to different generations of the homologous PPI dendrimer series gives a clear indication of the size dependent transition between realms of passive and active uptake of the exogeneous agents, effectively the transition between molecule and particle. Notably, although the basic chemical characteristics of the dendrimer generations are consistent and continuously varied, an abrupt transition from anti-oxidant (G0-G1) to oxidant action (>G2) is observed. G2 appears to be intermediate, as although early stage endosomes are observable (Figure 3), the substantially reduced toxicity elicited suggests that this is not the dominant uptake mechanism.

Elucidation of the critical importance of the endocytotic process for the cellular response to nanoparticle exposure, at least in the case of cationic nanoparticles, has implications for the development of predictive models and quantitative structure property relationships (QSARS) for nanoparticles, and even strategic approaches for nanomedical applications. There is a wealth of resources from the pharmaceutical field in terms of such models and QSARS which could potentially guide strategies for nanotoxicology and nanomedicine, many of which are available as open source tools (see for example http://www.opentox.org/). However, the study of the homologous PPI series indicates that, in considering the physico-chemical properties of the exposure species, the thresholds governing the uptake mechanism of the cell must be considered. The current study is a clear illustration that the initial, early phase oxidative stress observed for cationic nanoparticles is a result of the mechanism of processing the uptaken nanoparticles in endosomes, which struggle to digest them, causing extreme oxidative stress which can lead to apoptosis (Heiden et al., 2007). In some cases, the burden on endosomes can be extreme enough to cause endosomolysis (Kukowska-Latallo et al., 1996, Zhou et al. 2006, Guillot-Nieckowski et al., 2007) which itself can be disruptive to the cell (Mukherjee 2012). This strongly suggests that, in the case of cationic nanoparticles for intracellular nanomedical applications, avoiding the process of endocytosis may be a valid strategy to pursue (Guarnieri et al. 2014).

5 Conclusion

PPI dendrimers have been shown to elicit a systematic structurally dependent toxic response in human cells *in vitro*. The toxicity is dose and generation dependent, and the mechanism of response is consistent with that previously observed for PAMAM dendrimers of initial endocytosis, giving rise to early stage oxidative stress, release into the cytosol and a subsequent later stage of oxidative stress associated with the mitochondria. Of importance for potential biomedical applications, the similarity of the bi-phasic responses also indicates that, after initial encapsulation in endosomes, the dendrimer species, and any active cargo, become bioavailable after the first few hours. The observed correlation of the toxic responses for the higher generation dendrimers points towards the basis of structure activity relationships, but the differences between the responses of the PPI and PAMAM dendrimer series are indicative of a size dependent uptake mechanism, which should be considered in a generalised model.

The anomalous behaviour observed for the smaller PPI dendrimer generations indicates that alternative uptake pathways maybe accessible for the smaller species. Nanoparticles and in particular dendrimers are generally considered to cross cellular membranes by active transport mechanisms, particularly endocytosis, whereas smaller molecules can enter the cell by passive mechanisms. Identifying the threshold between the active uptake of the larger PPI generations G3 – G4, and the passive uptake of the smaller G0 and G1 dendrimers provides further insight into the mechanisms of nanotoxic responses and potential design strategies for nanomedicine. Although cationic nanoparticles are considered to be agents of oxidative stress, in this study it is demonstrated that the lower generations intrinsically act as anti-oxidants and the oxidative stress elicited by the higher generations is due to the endosomal and lysosomal pathway. The study suggests that strategies which can bypass the intrinsic cellular uptake processes may be appropriate for intracellular drug delivery. The study of the well-defined homologous PPI dendrimer series also indicates that, in considering the development of QSARS, thresholds of cellular uptake mechanisms must also be taken into consideration and that existing molecular based toxicity databases and predictive models may not be easily extendible to nanoparticle equivalents.

Acknowledgement:

This research was supported by the Integrated NanoScience Platform, Ireland (INSPIRE), funded under the Higher Education Authority PRTLI (Programme for Research in Third Level Institutions) Cycles 4 and 5, co-funded by the Irish Government and the European Union Structural fund.

References

Bhattacharyya T, Karnezis AN, Murphy SP, Hoang T, Freeman BC, Phillips B, Morimoto RI, 1995, Cloning and subcellular localization of human mitochondrial hsp70, *J Biol Chem* **270** 1705-1710

Bourne M.W., Margerun L., Hylton N., Campion B., Lai, J.J., Derugin N., Higgins C.B. 1996 Evaluation of the effects of intravascular MR contrast media (gadolinium dendrimer) on 3D time of flight magnetic resonance angiography of the body. *J. Magn. Reson. Imaging* **6**: 305–310.

Bouwmeester H., Lynch I., Marvin H.J.P., Dawson K.A., Berges M., Braguer D., Byrne H.J., Casey A., Chambers G., Clift M.J.D., Elia G., Fernandes T.F., Fjellsbo L.B., Hatto P., Juillerat L., Klein C., Kreyling W.G., Nickel C., Riediker M., Stone V. 2011 Minimal analytical characterization of engineered nanomaterials needed for hazard assessment in biological matrices, *Nanotoxicology*, **5**: 1-11

Cheng Y., Zhao L.,Li Y., Xu T., 2011 Design of biocompatible dendrimers for cancer diagnosis and therapy: current status and future perspectives. *Chem. Soc. Rev*, **40**: 2673–2703

Crooks RM, Zhao M, Sun L, Chechik V, Yeung LK. 2001 Dendrimer-encapsulated metal nanoparticles: synthesis, characterization, and applications to catalysis. *Acc Chem Res*. **34**: 181-90.

Dahle JT, Arai Y. 2015. Environmental geochemistry of cerium: applications and toxicology of cerium oxide nanoparticles. *Int J Environ Res Public Health*, **12**: 1253-1278.

Dear, J.W., Kobayashi, H., Brechbiel M.W., Star R.A., 2006 Imaging acute renal failure with polyamine dendrimer-based MRI contrast agents. *Nephron Clin Pract* **103** : c45-c49.

Duncan R., Izzo L. 2005 Dendrimer biocompatibility and toxicity. *Adv. Drug Deliv. Rev.* **57**: 2215– 2237.

Ekkapongpisit M, Giovia A, Follo C, Caputo G, Isidoro C. 2012 Biocompatibility, endocytosis, and intracellular trafficking of mesoporous silica and polystyrene nanoparticles in ovarian cancer cells: effects of size and surface charge groups. *Int J Nanomedicine* **7**: 4147-58

Gajraj A., Ofoli, R.Y., 2000. Effect of extrinsic fluorescent labels on diffusion and adsorption kinetics of proteins at the liquid–liquid interface. *Langmuir* **16**, 8085–8094.

Guarnieri D, Sabella S, Muscetti O, Belli V, Malvindi MA, Fusco S, De Luca E, Pompa PP, Netti PA. 2014 Transport across the cell-membrane dictates nanoparticle fate and toxicity: a new paradigm in nanotoxicology. *Nanoscale* **6**: 10264-10273.

Guillot-Nieckowski M., Eisler S., Diederich F., 2007 Dendritic vectors for gene transfection. *New J. Chem.* **31**: 1111–1127.

Heiden TC., Dengler E., Kao WJ., Heideman W., Peterson RE., 2007. Developmental toxicity of low generation PAMAM dendrimers in zebrafish. *Toxicol Appl Pharmacol*. **225:** 70-79.

Hipkiss AR. 2009 Carnosine and its possible roles in nutrition and health. *Adv Food Nutr Res.* **57**: 87-154.

Janaszewska A., Mączyńska K., Matuszko G., Appelhans D., Voit B., Klajnert B. and Bryszewska M., 2012 Cytotoxicity of PAMAM, PPI and maltose modified PPI dendrimers in Chinese hamster ovary (CHO) and human ovarian carcinoma (SKOV3) cells. *New J. Chem.* **36:** 428-437.

Kannan RM, Nance E, Kannan S, Tomalia DA. 2006 Emerging concepts in dendrimer-based nanomedicine: from design principles to clinical applications. *J Intern Med.* **276**: 579-617.

Kehrer JP, Paraidathathu T, 1992, The use of fluorescent probes to assess oxidative processes in isolated-perfused rat heart tissue. *Free Radic Res Commun.* **16** 217-25.

Kesharwani P, Tekade RK, Jain NK. 2014 Generation dependent cancer targeting potential of poly(propyleneimine) dendrimer. *Biomaterials* **35**: 5539-48.

Kesharwani P, Iyer AK. 2015 Recent advances in dendrimer-based nanovectors for tumor-targeted drug and gene delivery. *Drug Discov Today* **20**: 536-47

Kesharwani P., Tekade R.K., Jain N.K. 2015 Dendrimer generational nomenclature: the need to harmonize, *Drug Discov Today*, **20**: 497-499

Kitchens KM., Kolhatkar RB., Swaan PW., Ghandehari H. 2008 Endocytosis inhibitors prevent poly(amidoamine) dendrimer internalization and permeability across Caco-2 cells. *Mol. Pharm.* **5**: 364–369.

Kost, T.A., Patrick J. 1999 Recombinant baculoviruses as expression vectors for insect and mammalian cells, *Current Opinion in Biotechnology* **10**: 428-433.

Kukowska-Latallo JF, Bielinska AU, Johnson J, Spindler R, Tomalia DA, Baker JR Jr. 1996 Efficient transfer of genetic material into mammalian cells using Starburst polyamidoamine dendrimers. *Proc. Natl. Acad. Sci.* **93**: 4897-902.

Lee JH., Cha KE., Kim MS., Hong HW., Chung DJ., Ryu G., Myung H. 2009 Nanosized polyamidoamine (PAMAM) dendrimer induced apoptosis mediated by mitochondrial dysfunction. *Toxicol Lett.* **190**: 202-207.

Liu R, Lal R. 2015. Potentials of engineered nanoparticles as fertilizers for increasing agronomic productions. *Sci Total Environ.* **514**:131-139.

Lotito SB, Frei B. 2004 Relevance of apple polyphenols as antioxidants in human plasma: contrasting *in vitro* and *in vivo* effects. *Free Radic Biol Med.* **36** 201-211.

Lynch I, Ahluwalia A, Boraschi D, Byrne HJ, Fadeel B, Gehr P, Gutleb AC, Kendall M, Papadopoulos MG. 2013. The bio-nano-interface in predicting nanoparticle fate and behaviour in living organisms: towards grouping and categorising nanomaterials and ensuring nanosafety by design. *BioNanoMaterials*. **14:** 195–216

Maher M.A.., Naha P.C., Mukerjee S.P., Byrne H.J. 2014 Numerical simulations of *in vitro* nanoparticle toxicity – the case of Poly(amido amine) dendrimers *Tox. in Vitro*, **28**: 1449-1460

Monti DM, Guarnieri D, Napolitano G, Piccoli R, Netti P, Fusco S, Arciello A. 2015 Biocompatibility, uptake and endocytosis pathways of polystyrene nanoparticles in prima ry human renal epithelial cells. *J Biotechnol.* **193**: 3-10.

Mozdzan M, Szemraj J, Rysz J, Stolarek RA, Nowak D. 2006 Anti-oxidant activity of spermine and spermidine re-evaluated with oxidising system involvoing iron and copper ions. *Int J Biochem Cell Biol.* **38**: 69-81.

Mukherjee SP, Byrne HJ 2010 In vitro mammalian cytotoxicological study of PAMAM dendrimers -towards quantitative structure activity relationships, *Tox. in Vitro*, **24**: 169-177

Mukherjee SP., Lyng FM., Garcia A., Davoren M., Byrne HJ., 2010. Mechanistic studies of in vitro cytotoxicity of poly(amidoamine) dendrimers in mammalian cells. *Toxicol Appl Pharmacol*. **248**: 259-268.

Mukherjee S.P, 2012 *PhD Thesis*, Dublin Institute of Technology

Mukherjee SP, Byrne HJ 2013 Polyamidoamine Dendrimer Nanoparticle Cytotoxicity, Oxidative Stress, Caspase Activation and Infammatory Response: Experimental Observation and Numerical Simulation. *Nanomedicine* **9**: 202-211.

Naha PC, Davoren M, Lyng FM, Byrne HJ 2010 Reactive oxygen species (ROS) induced cytokine production and cytotoxicity of PAMAM dendrimers in J774A.1 cells. *Toxicol Appl Pharmacol.* **246**: 91-99.

Naha PC., Byrne HJ. 2013 Generation of Intracellular Reactive Oxygen Species and Genotoxicity effect to Exposure of Nanosized Polyamidoamine (PAMAM) dendrimers in PLHC-1 cells in vitro. *Aquat. Toxicol.* **132– 133**: 61– 72.

Najlah M., D'Emanuele A. 2006 Crossing cellular barriers using dendrimer nanotechnologies. *Curr Opin Pharmacol.* **6**: 522-527.

Nel, A., Xia, T., Madler, L., Li, N. 2006 Toxic potential of materials at the nanolevel. *Science* **311**: 622–627.

Nel, A.E., Mädler, L., Velegol, D., Xia, T., Hoek, E.M.V., Somasundaran, P., Klaessig, F., Castranova, V. and Thompson, M. 2009 Understanding biophysicochemical interactions at the nano–bio interface. *Nat. Mater.* **8**: 543 - 557

Oomen A, Bos P, Fernandes T, Hund-Rinke K, Boraschi D, Byrne HJ, Aschberger K, Gottardo S, von der Kammer F, Kühnel D, Hristozov D, Marcomini A, Migliore L, Scott-Fordsmand J, Wick P, Landsiedel R. 2014. Concern-driven integrated toxicity testing strategies for nanomaterials - Report of the NanoSafety Cluster Working Group 10. *NanoToxicology* **8**: 334-338.

Parat A, Bordeianu C, Dib H, Garofalo A, Walter A, Bégin-Colin S, Felder-Flesch D. 2015. Dendrimer-nanoparticle conjugates in nanomedicine. *Nanomedicine* **10**: 977-992.

Perumal OP., Inapagolla R., Kannan S., Kannan RM., 2008 The effect of surface functionality on cellular trafficking of dendrimers. *Biomaterials* **29**: 3469–3476

Pignatello, R., Musumeci, T., Impallomeni, G., Carnemolla, G.M., Puglisi, G., Ballistreri, A. 2009 Poly(3-hydroxybutyrate-co-epsilon-caprolactone) copolymers and poly(3-hydroxybutyrate-co-3-hydroxyvalerate-co-epsilon-caprolactone) terpolymers as novel materials for colloidal drug delivery systems. *Eur. J. Pharm. Sci.* **37**: 451–462.

Project on Emerging Nanotechnologies (PEN) http://www.nanotechproject.org/ [20th Sept 2015]

Ragnvaldsson, D., Berglind, R., Tysklind, M., Leffler P., 2007 Environmental hazard screening of a metal-polluted site using pressurized liquid extraction and two in vitro bioassays. *J. Hum. Environ.* **36 :** 494–501.

Salvati A., Aberg C., dos Santos T., Varela J., Pinto P., Lynch I., Dawson KA., 2011 Experimental and theoretical comparison of intracellular import of polymeric nanoparticles and small molecules: toward models of uptake kinetics. *Nanomedicine* **7**: 818-826.

Sandin P, Fitzpatrick LW, Simpson JC, Dawson KA. 2012 High-speed imaging of Rab family small GTPases reveals rare events in nanoparticle trafficking in living cells. *ACS Nano*. **6**: 1513-21.

Saovapakhiran A, D'Emanuele A, Attwood D, Penny J. 2009 Surface modification of PAMAM dendrimers modulates the mechanism of cellular internalization. *Bioconjug. Chem.* **20**: 693-701.

Shao N, Su Y, Hu J, Zhang J, Zhang H, Cheng Y. 2011 Comparison of generation 3 polyamidoamine dendrimer and generation 4 polypropylenimine dendrimer on drug loading, complex structure, release behaviour, and cytotoxicity. *Int. J. Nanomed.* **6**: 3361–3372

Swanson S. D., Kukowska-Latallo J. F., Patri A. K., Chen C., Ge S., Cao Z., Kotlyar A., East A.T., Baker J. R., 2008 Targeted gadolinium-loaded dendrimer nanoparticles for tumor-specific magnetic resonance contrast enhancement. *Int. J. Nanomed*. **3**: 201-210

Thomas T.P., Majoros I., Kotlyar A., Mullen D., Holl M.M.B., Baker J.R., 2009. Cationic poly(amidoamine) dendrimer induces lysosomal apoptotic pathway at therapeutically relevant concentrations. *Biomacromolecules* **10**, 3207–3214.

Tomalia DA., 2005 Birth of a new macromolecular architecture: dendrimers as quantized building blocks for nanoscale synthetic polymer chemistry. *Prog Polym Sci.* **30**: 294–324.

Tomalia D.A. and Rookmaker M. 2009 *Polymer Data Handbook* (Mark, J.E., ed.), Oxford University Press, 979–982

Twyman, L.J., Beezer, A.E., Esfand, R., Hardy, M.J., Mitchell, J.C. 1999 The synthesis of water soluble dendrimers, and their application as possible drug delivery systems. *Tetrahedron Lett*. **40**: 1743–1746.

van Meerloo J, Kaspers GJ, Cloos J. 2011 Cell sensitivity assays: the MTT assay. *Methods, Mol Biol.* **731**: 237-45.

Varkouhi AK., Scholte M., Storm G., Haisma HJ., 2011 Endosomal escape pathways for delivery of biologicals. *J Control Release* **151**: 220-228.

Wang LH., Rothberg KG., Anderson RG. 1993 Mis-assembly of clathrin lattices on endosomes reveals a regulatory switch for coated pit formation. *J. Cell Biol.* **123:** 1107–1117.

Wang F., Cai X., Su Y., Hu J., Wu Q., Zhang H., Xiao J., Cheng Y., 2012 Reducing cytotoxicity while improving anti-cancer drug loading capacity of polypropylenimine dendrimers by surface acetylation. *Acta Biomaterialia* **8**: 4304–4313

Xia T., Kovochich M., Brant J., Hotze M., Sempf J., Oberley T., Sioutas C., Yeh JI., Wiesner MR., Nel AE. 2006 Comparison of the abilities of ambient and manufactured nanoparticles to induce cellular toxicity according to an oxidative stress paradigm. *Nano Lett.* **6**: 794-807.

Zhou J., Wu J., Hafdi N., Behr J.P., Erbacher P., Peng, L. 2006 PAMAM dendrimers for efficient siRNA delivery and potent gene silencing. *Chem. Comm.* **22**: 2362-2364.

Figure Captions

Figure 1. Dose dependent cytotoxicity, as determined using the MTT assay after 24hrs exposure of HaCaT cells to PPI G0, G1, G2, G3 and G4 dendrimers. Error bars indicate the standard deviation of three individual measurements, each containing six replicates. The solid lines are a fit to the experimental data, as described in Section 2.6.

Figure 2. ROS production compared to control in HaCaT cells treated with PPI dendrimers G0, G1 and G4 over a 24hr period at EC_{50} concentrations determined by the MTT assay.

Figure 3: Confocal image of HaCaT cells exposed to PPI dendrimers in the presence of Carboxy H_2DCFDA dye (yellow) and mitotracker dye (red). (a) PPI G2 20μM after 5hrs exposure, (b) PPI G2 20μM after 24hrs exposure. The dominance of the red mitotracker dye indicates the absence of ROS in the mitochondria is (a) after 5hrs, whereas the orange colour in (b) indicates colocatisation of ROS in the mitochondria after 24hrs.

Figure 4: Confocal image of HaCaT cells after 5hr exposure to 0.3μM PPI G4 in the presence of CellLight dye (red). (a) CellLight fluorescence indicating the presence of early endosomes, (b) phase contrast image. (c) overlap of early endosome fluorescence and phase contrast image.

Figure 5: Confocal image of HaCaT cells exposed to 1000μM PPI G0 in the presence of CellLight reagent after 5hrs exposure. (a) absence of CellLight fluorescence indicating the absence of early endosomes, (b) phase contrast image. (c) overlap of early endosome fluorescence and phase contrast image.

Figure 6. Comparison of EC_{50} values of PPI G0 – G4 dendrimers with those of PAMAM G4- G6, as measured by the MTT assay in the HaCaT cell line after 24hrs exposure. Error bars indicate the standard deviation of three individual measurements, each containing six replicates. Solid lines are a guide to the eye.

Figure 7. Comparison of early maximum ROS in relation to surface amino groups of PPI G0 – G4 and PAMAM G4 – G6. Error bars are the standard deviation of three independent experiments, each including six replicates of each treatment concentration. The solid line is a guide to the eye.

Figure 8. Early stage % ROS production vs Inverse EC_{50} (24hrs) of PPI and PAMAM in HaCaT cells at EC_{50} values of PPI and PAMAM determined by the MTT assay. Error bars (ROS) are the standard deviation of three independent experiments, each including six replicates of each treatment concentration. The solid line is a guide to the eye.

745

746 **Figure 1:**

747
748
749
750
751
752
753
754
755
756
757
758
759
760
761
762
763
764
765
766
767
768
769
770
771
772
773
774
775

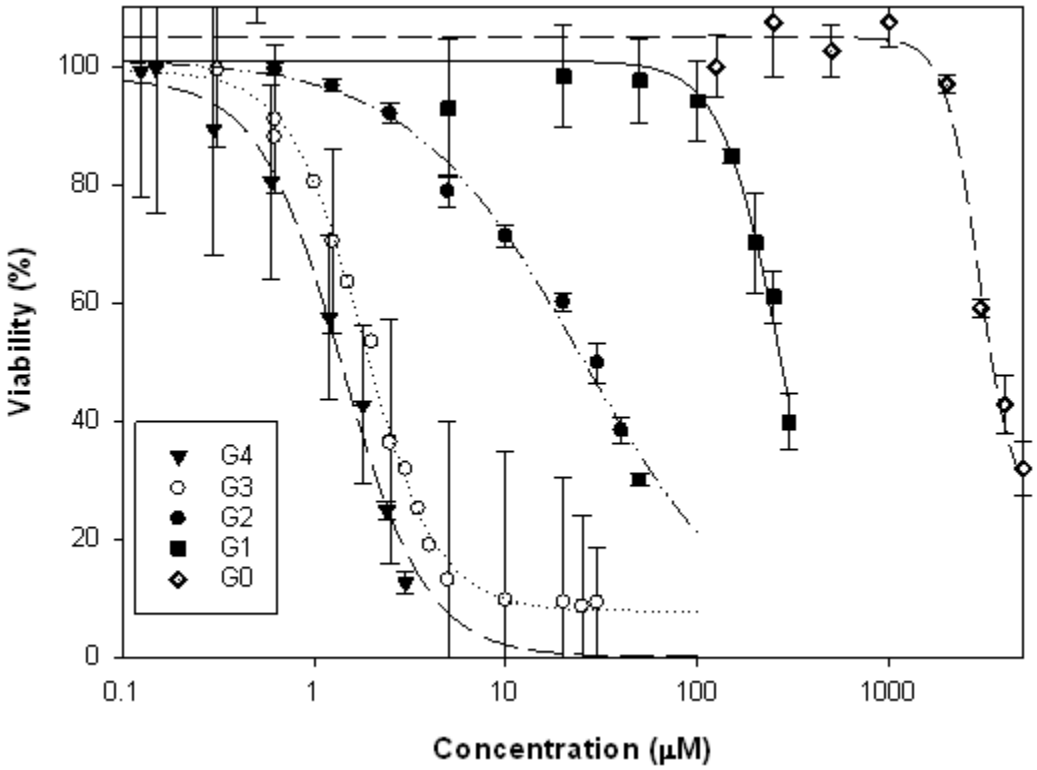

776
777

Figure 2:

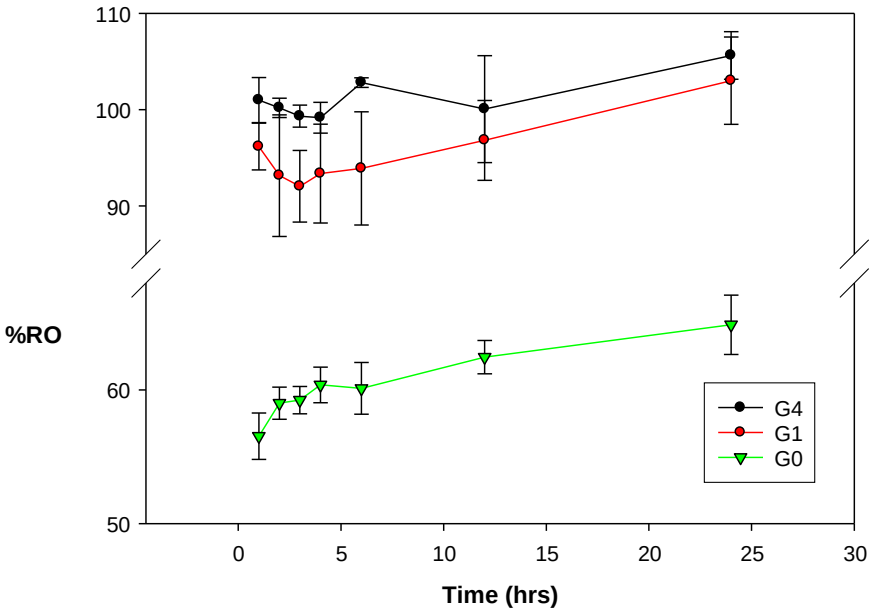

Figure 3:

(a) (b)

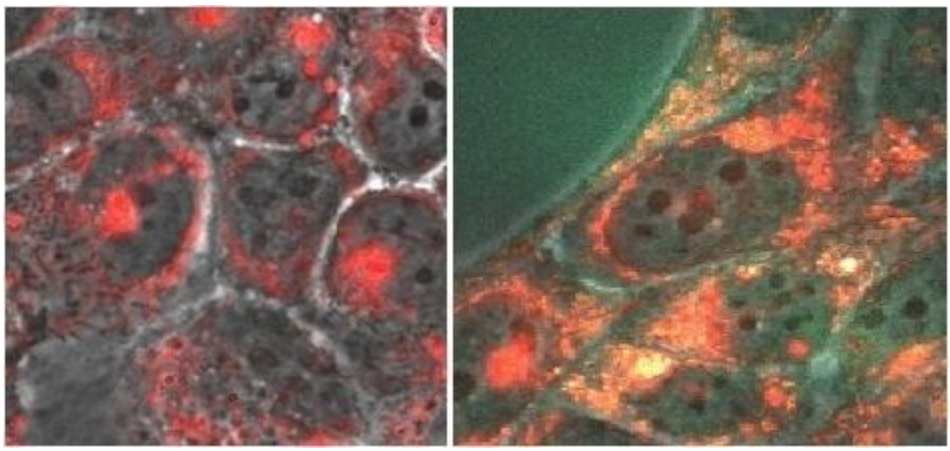

804 **Figure 4:**

805

806

807

808

809

810 (a) (b)

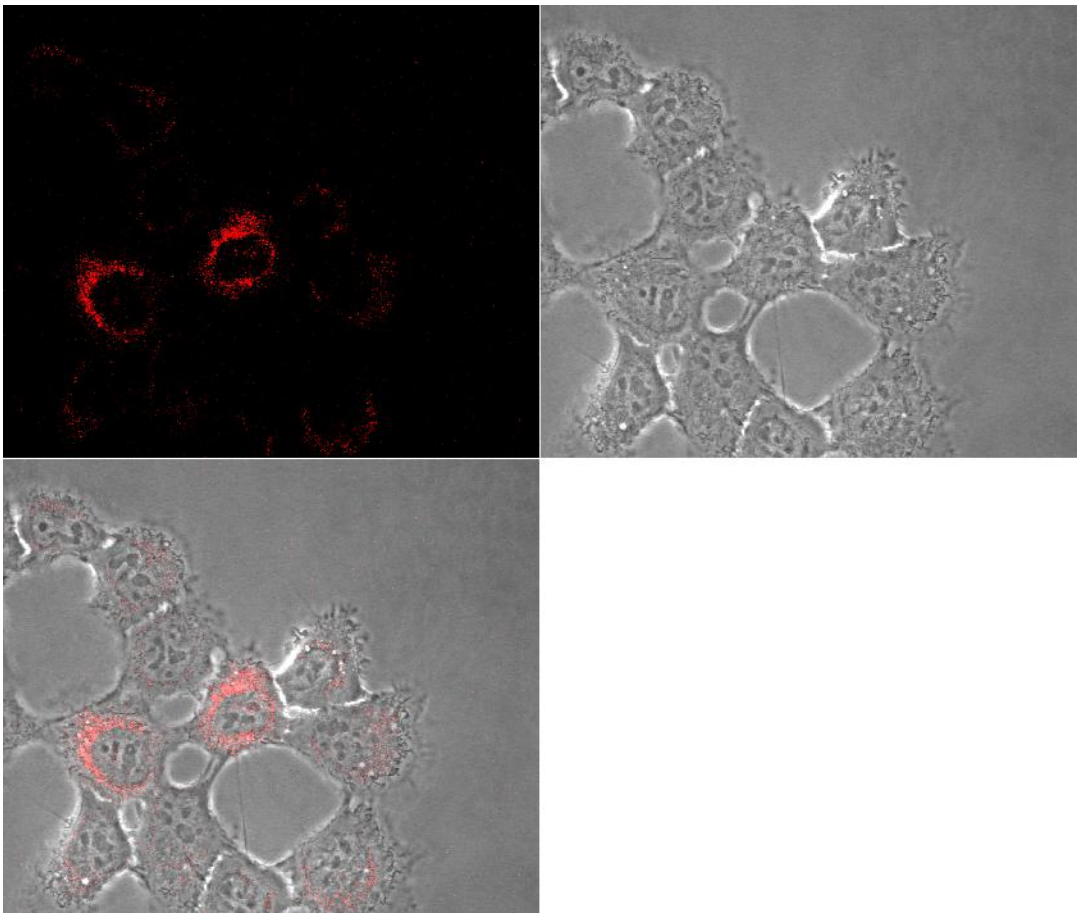

811

812 (c)

813

814

Figure 5:

(a) (b)

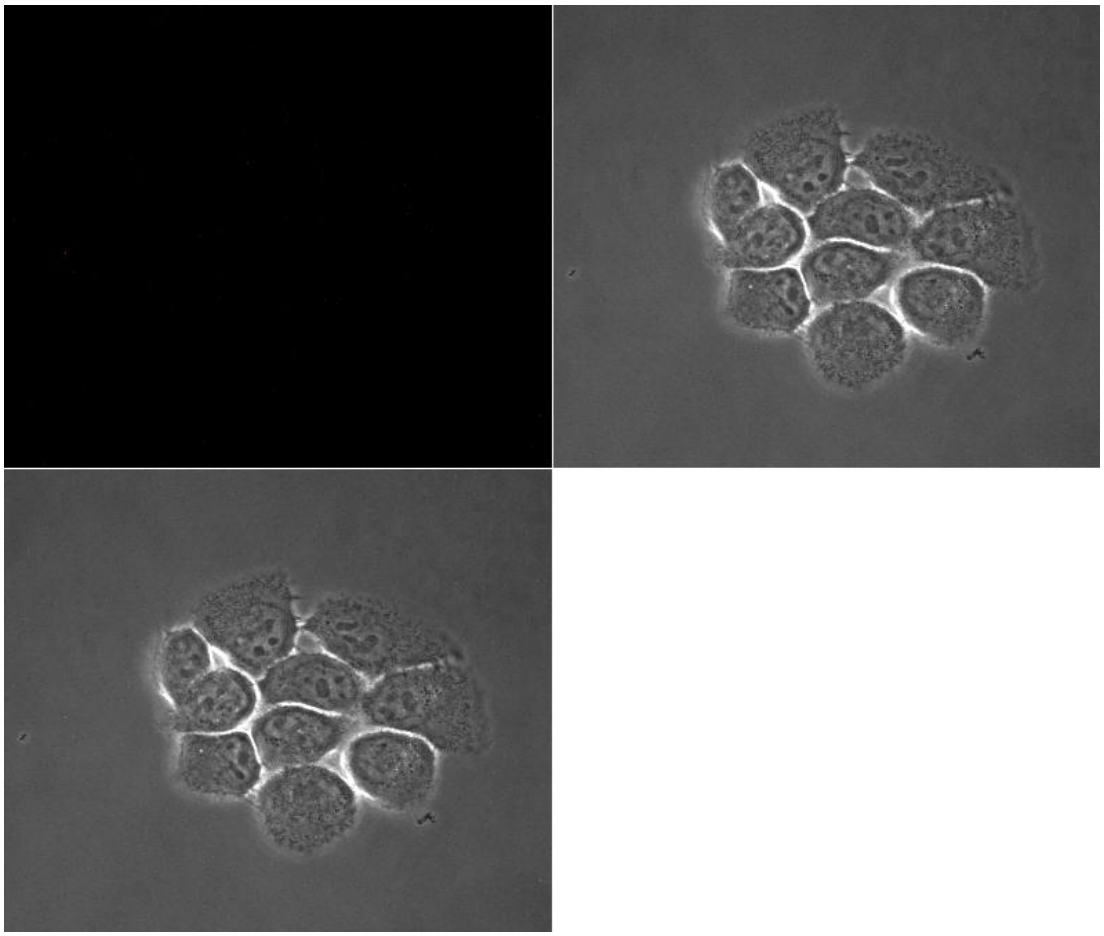

(c)

Figure 6:

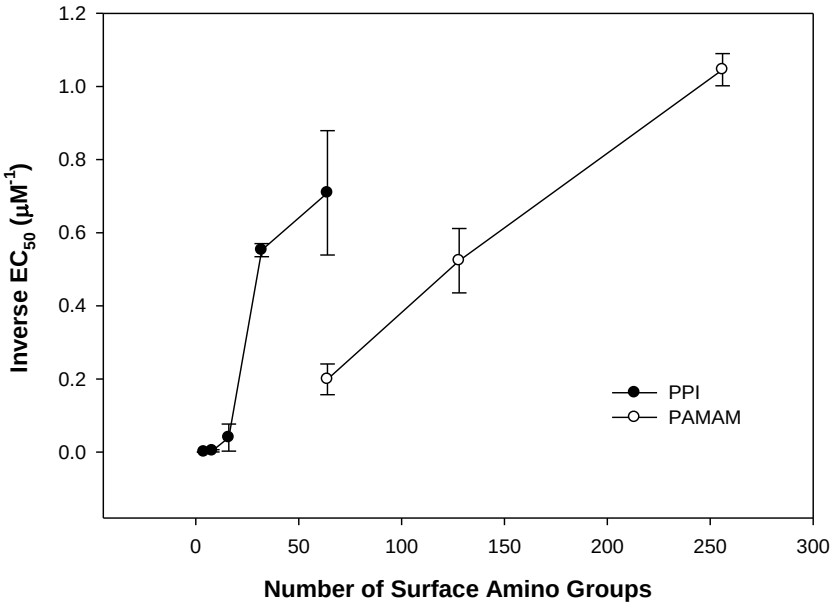
1.2
1.0
0.8
0.6
0.4
0.2
0.0
Inverse EC50 (μM-1)
0
50
100
150
200
250
300
Number of Surface Amino Groups
PPI
PAMAM

Figure 7:

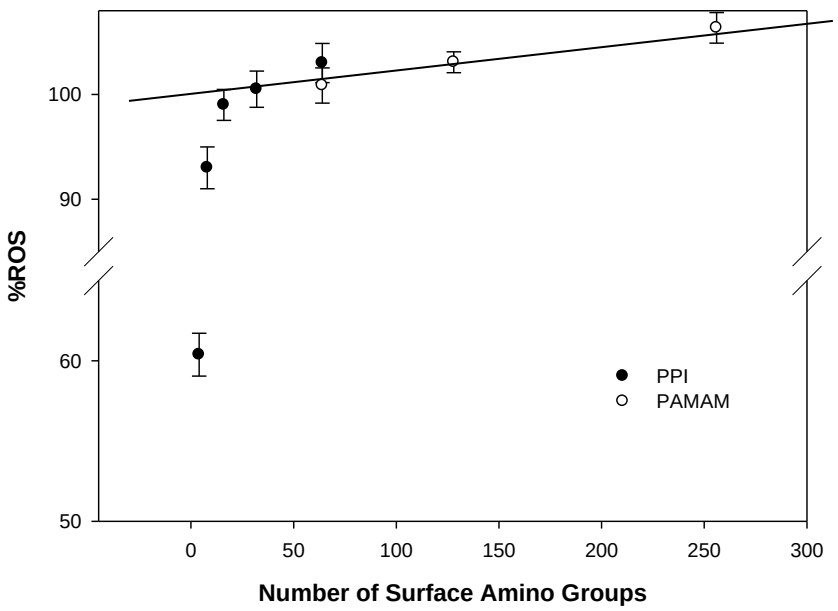
%ROS
100
90
60
50
0
50
100
150
200
250
300
Number of Surface Amino Groups
PPI
PAMAM

Figure 8:

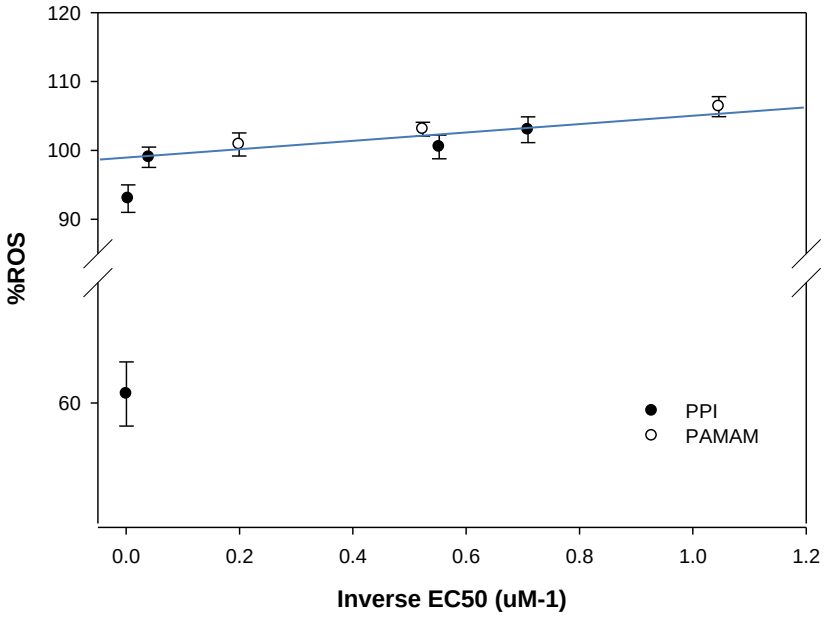
120
110
100
90
60
%ROS
0.0
0.2
0.4
0.6
0.8
1.0
1.2
Inverse EC50 (uM-1)
PPI
PAMAM

	Molecular Weight (grams per mole)	Number of Surface Amino Groups	Particle size (Crooks et al. 2001) (nm)	Particle size (AFM) (nm)	EC_{50}(µM)
PPI – G4	7,168	64	2.8	2.5-3.5	1.41 ± 0.3
PPI – G3	3,514	32	2.4	1.8-2.6	1.81 ± 0.3
PPI – G2	1,687	16	1.9 [2.4]	1.7-1.9	24.8 ± 3.75
PPI – G1	773.3	8	[1.8]	2 – 8*	271.04 ± 33.5
PPI – G0	316.5	4	[1.23]	4 – 10*	2939.72 ± 191
PAMAM – G6	58,408	256	6.7	4.2-5.8	1.02 ± 0.3
PAMAM – G5	28,826	128	5.4	4.1-4.6	1.91 ± 0.28
PAMAM – G4	14,215	64	4.5	2.1-2.8	5.02 ± 0.29

Table 1. Comparison of the structural characteristics and cytotoxic responses of PPI and PAMAM dendrimers. [] indicates size as determined by the Hyperchem geometrical optimised model (See supplemental Material). * indicates that particle aggregation was observed